Premature Senescence Leaf 50 Promotes Heat Stress Tolerance in Rice (Oryza Sativa L.)

Yan He
China National Rice Research Institute
Xiao-bo Zhang
China National Rice Research Institute
Yongfeng Shi
China National Rice Research Institute
Xia Xu
China National Rice Research Institute
Liangjian Li
China National Rice Research Institute
Jian-li Wu (beishangd@163.com)
China National Rice Research Institute https://orcid.org/0000-0003-3480-1503

Short communication

Keywords: Rice, Senescence, IMBR, Heat tolerance, Hydrogen peroxide

Posted Date: December 3rd, 2020

DOI: https://doi.org/10.21203/rs.3.rs-116224/v1

Abstract

Background

Heat stress is a major environmental factor that could induce premature leaf senescence in plants. So far, few rice premature senescent leaf mutants have been reported to involve in heat tolerance.

Findings

We identified a *premature senescence leaf 50* (*psl50*) mutant that exhibited a higher heat susceptibility with decreased survival rate, over-accumulated hydrogen peroxide (H_2O_2) content and increased cell death under heat stress compared with the wild-type. The causal gene *PREMATURE SENESCENCE LEAF 50* (*PSL50*) was isolated by using initial map-based resequencing (IMBR) approach, and we found that *PSL50* promoted heat tolerance probably by acting as a modulator of H_2O_2 signaling in response to heat stress in rice (*Oryza sativa* L.).

Conclusions

PSL50 negatively regulates heat-induced premature leaf senescence in rice.

Findings

In plants, premature leaf senescence is a major symptom resulting from heat stress. During heat-induced senescence, leaf cells undergo a series of cellular changes including reactive oxygen species (ROS) accumulation, photosynthetic apparatus impairment and cell death (Cui et al. 2020; Ivanov et al. 2017; Lee et al. 2014). Accordingly, plants have developed complex biochemical regulatory mechanisms to response and adapt to heat stress (Samakovli et al. 2020; Li et al. 2020; Wu et al. 2018). However, the underlying genetic and molecular mechanisms are largely unknown.

We previously characterized physio-biochemically an ethyl methane sulfonate (EMS) induced Zhongjian 100 (wild type, WT) mutant, *premature senescence leaf 50* (*psl50*), which displayed severe premature senescent phenotype at the grain-filling stage (Fig. 1a) (He et al. 2018).

To rapidly isolate the causal gene *PSL50* responsible for the premature senescent phenotype, we designed an initial map-based resequencing (IMBR) strategy to locate the candidate gene by combining initial mapping and whole-genome resequencing (Fig. 1b). To perform IMBR, *PSL50* was firstly mapped to a large region covering several megabit nucleotides after the initial mapping using a small F_2 population. Secondly, *psl50* and three randomly chosen mutants (*M1*, *M2* and *M3*) from the same mutant bank were sampled for whole-genome resequencing. Lastly, the sequences of the target initial mapping region from the four lines were aligned and compared with the reference genome of indica rice Minghui 63 (MH63, http://rice.hzau.edu.cn/cgi-bin/gb2/gbrowse/MH63RS2/) (Zhang et al. 2016) to detect SNP and/or InDel variations. It is not necessary to sequence WT because the sequences of four mutant lines can be used as control or biological replicates to lower/eliminate sequencing errors.

As a proof of concept, a total of 178 polymorphic simple sequence repeat (SSR) markers evenly distributed over 12 chromosomes between parental line *psl50* and japonica line 80A90YR72 were used for linkage analysis of two bulked segregant analysis (BSA) DNA pools derived from the wild-type and mutant type F_2 progenies from the cross *psl50*/80A90YR72. The results showed that three SSR markers RM297, RM443 and RM488 were co-segregated with the mutation. Further mapping indicated that *PSL50* localized to a 2.7-Mb genomic region between RM3411 and RM1297 at the long arm of chromosome 1 by using 40 *psl50*-type F_2 individuals derived from the cross *psl50*/80A90YR72 (Fig. 1c). Sequence alignments of the 2.7-Mb region showed that there were 155, 162 and 158 SNPs/InDels between *psl50/M1*, *psl50/ M2* and *psl50/M3*, respectively (Additional file 2: Table S1-S3). Obviously, most SNPs/InDels presented two types of genotype between *psl50* and the other three mutants, we cannot consider them as the true SNPs/InDels. Only the site(s) showing a single genotype at all allele depth was considered as true SNPs/InDels. As shown in Table S1-S3, only the position at 28,281,174 within the third exon of *LOC_Os01g50770* exhibited the nucleotide change from GC to G with single genotype in allele depth among all the sequence alignments between *psl50* (G/G with 0,24 allele depth) and the other three mutants (GC/GC with 10,0 allele depth for *M1*, 14,0 for *M2* and 18,0 for *M3*, respectively). These results revealed that the variation from GC to G at the position 28,281,174 was a true 1-bp deletion mutation in *LOC_Os01g50770* (Table 1; Fig. 1c).

We further performed sequencing on polymerase chain reaction (PCR) products to confirm the 1-bp deletion mutation which leads to a premature stop codon (Fig. 1c; Additional file 1: Figure S1a). *LOC_Os01g50770* is predicted to encode a clathrin-associated adaptor protein complex 1 medium subunit μ1 (AP1M1). The mutation type *LOC_Os01g50770* is predicted to encode a truncated protein (ΔPSL50) lacking the AP-1 complex subunit μ N-terminal domain, and the functional domain deletion could be observed visually by modeling the three-dimensional protein structures of PSL50 and ΔPSL50 (Additional file 1: Figure S1b, c). To quickly demonstrate whether the mutation of *LOC_Os01g50770* was responsible for premature leaf senescence in *psl50*, we transformed a CRISPR/Cas9 construct targeting the first exon of *LOC_Os01g50770* into a japonica rice variety Kitaake, rather than performing the complementation of *psl50* due to the recalcitrant nature in genetic transformation of indica rice (Fig. 1d). Expectedly, all 13 knockout homozygous lines of T_0 transgenic plants showed premature senescence leaf phenotype similar to *psl50* (Fig. 1e). These results confirmed that *LOC_Os01g50770* was *PSL50*, and the mutation of *PSL50* caused the premature senescence leaf phenotype in *psl50.* Furthermore, we also successfully identified other true mutations in the three control mutants (data not shown), indicating the feasibility of IMBR strategy in rapid gene solation.

Table 1. Nucleotide comparison of target mutation site between *psl50* and the other three mutants.

Material	Position	Genotype	Mutant depth	Mutant allele depth	Mutation type
psl50	28,281,174	G	10	10,0	GC to G (frameshift)
M1	28,281,174	GC	14	14,0	GC (wild-type)
M2	28,281,174	GC	18	18,0	GC (wild-type)
M3	28,281,174	GC	24	24,0	GC (wild-type)
MH63	28,281,174	GC			GC

Many senescence-associated mutants have been identified in various plant species (Liang et al. 2014; Zhao et al. 2016; Shim et al. 2019), while most of the studies focused on the interpretation of senescence-related genetic mechanisms. To explore the association between environmental factors and premature leaf senescence, we carried out a heat treatment on *psl50* at the seedling stage. Under normal growth conditions at 26°C, no any overt abnormalities or defects were observed in *psl50* compared with WT. However, when 12-day-old seedlings were subjected to heat treatment at 45°C under hydroponics and soil growth conditions, *psl50* showed more susceptible to heat stress and lower survival rate than those of WT (Fig. 2a, c). Hydrogen peroxide (H_2O_2) over-accumulation is shown to induce plant cell death (He et al. 2020; Sathe et al. 2019). We hence detected H_2O_2 accumulation and cell death of *psl50* seedlings with and without heat treatment by using 3,3'-diaminobenzidine (DAB) and trypan blue staining. The results showed that *psl50* had similar level of H_2O_2 accumulation and cell death before heat treatment at 26°C, whereas *psl50* had higher levels of H_2O_2 accumulation and cell death after heat treatment at 45°C compared with WT (Fig. 2b, d). Although ion leakage rate was dramatically increased both in WT and *psl50* after heat treatment, *psl50* showed significantly increased ion leakage rate compared to WT (Fig. 2e). As another indicator of cell membrane damage, the malonaldehyde (MDA) content was similar between *psl50* and WT before heat treatment, while obviously increased in *psl50* after heat treatment (Fig. 2f). These results indicated that *PSL50* could positively contribute to heat tolerance, while dysfunction of *PSL50* in *psl50* resulted in higher heat stress susceptibility associated with cell membrane damage and H_2O_2-induced cell death. In addition, the H_2O_2 content was similar in green leaves of WT and *psl50*, while prominently increased in premature senescent leaves of *psl50* (Additional file 1: Figure S2). Considering rapid premature leaf senescence occurred in *psl50* at the grain-filling stage which often accompanied with higher temperatures in natural conditions, we speculated that high temperatures might act as an inducer for premature leaf senescence in *psl50*, involving H_2O_2 signaling response pathway.

PSL50 is likely allelic to *SPOTTED LEAF 28* (*SPL28*) in rice, which is involved in the regulation of vesicular trafficking (Qiao et al. 2010). To detect the subcellular location of PSL50, we fused the green fluorescent protein (GFP) to the C-terminus of PSL50 driven by the CaMV35S promoter to create the PSL50::GFP fusion protein. The PSL50::GFP fluorescent signals were co-localized with NST1::mCherry, a Golgi-tagged marker (Zhang et al. 2011), indicating that PSL50 localized to the Golgi apparatus (Fig. 3a), and this result was consistent with the subcellular localization of SPL28 in onion epidermal cells (Qiao et al. 2010). The expression of *PSL50* was detectable in all different rice organs at different developmental

stages, and its expression increased gradually from the top to the base of a fully expanded flag leaf (Fig. 3b, c). In addition, we examined *PSL50* expression in different leaves at the mature stage, and found that *PSL50* transcripts were higher in younger, greener leaves than those of older and senescing leaves (Additional file 1: Figure S3). The results suggested that *PSL50* was widely expressed and acted as a negative regulator for natural rice leaf senescence. To explore the roles of *PSL50* in heat tolerance, we further investigated the kinetic mRNA level alterations of *PSL50* in WT and *psl50* under heat stress conditions. In WT, *PSL50* mRNA levels decreased by 0.4-fold after 2 h heat treatment, and increased rapidly by 2.4-fold after 4 h, whereas in *psl50*, a similar variation trend of *PSL50* mRNA levels emerged after 6 h heat treatment (Fig. 3d). The results indicated that *PSL50* transcription was induced by heat stress and the compromised heat tolerance of *psl50* may be not only the consequence of *PSL50* mutation but also the delayed expression response of *PSL50* in *psl50*.

We also detected the transcripts of ROS-scavenging system associated genes, including ascorbate peroxidase gene *OsAPX1*, *OsAPX2* (Bonifacio et al. 2016), catalase gene *OsCATA*, *OsCATB*, *OsCATC* (Lin et al. 2012; Ye et al. 2011), alternative oxidase gene *OsAOX1a*, *OsAOX1b*, *OsAOX1c* (Fujii et al. 2008; Saika et al. 2002), and superoxide dismutase gene Cu/Zn-SOD, Mn-SOD, Fe-SOD (Wang et al. 2016; Guan et al. 2017). In contrast to the normal growth conditions at 26°C, *OsAPX2*, *OsCATC*, *Mn-SOD* and *Fe-SOD* were significantly up-regulated, while *OsCATB*, *OsAOX1a*, *OsAOX1b* and *OsAOX1c* were dramatically down-regulated in *psl50* after heat treatment (Fig. 3e). These results indicated that the H_2O_2 accumulation in *psl50* under heat stress was regulated at a transcriptional level of ROS-scavenging system associated genes. In plants, H_2O_2 is mainly produced in thylakoids during the light reaction of photosynthesis (Asada, 2006). Thus, immunoblot was performed to test whether the major components of thylakoid membrane complexes were impaired under heat stress. As the core subunits of photosystem (PS) II and I complexes, PsaB and PsbD were dramatically decreased in both WT and *psl50* after 45°C heat treatment (Fig. 3f). However, the accumulations of light-harvesting antenna of PSI (LHCI) chlorophyll *a*/*b*-binding proteins Lhca1, 2, 4 and NAD(P)H dehydrogenase subunit5 (NdhF) were not affected by heat treatment, even slightly increased in *psl50* compared to WT after heat treatment. Compared with WT, the levels of LHCII type II chlorophyll *a*/*b*-binding protein Lhcb2 and ATP synthase *β*-subunit (AtpB) showed slight weakening in *psl50* after heat treatment (Fig. 3f). The immunoblot assay suggested that impairments of thylakoid membrane complex proteins under heat stress might result in H_2O_2 over-accumulation as integral thylakoids are essential for H_2O_2 scavenging in photosynthetic light reaction.

Taken together, we successfully identified and isolated rice *PSL50* by using the IMBR strategy. Additionally, we found that PSL50 played important roles both in rice premature leaf senescence and heat stress response, involving in the regulation of H_2O_2 accumulation. This study would facilitate studies on functions of PSL50 in heat stress-induced premature leaf senescence.

Materials And Methods

Plant materials and growth conditions

The *psl50*, mutant1 (*M1*), mutant2 (*M2*), mutant3 (*M3*) were obtained from an EMS-induced indica rice accession Zhongjian100 (wild-type, WT) mutant bank. The four mutants, wild-type and F_2 individual plants from the cross *psl50*/80A90YR72 were grown in the paddy field at the China National Rice Research Institute (CNRRI). For the heat treatment, plants were cultured respectively with soil and hydroponically cultured with Yoshida rice nutrient salt mixture (Coolaber, NSP1040) after germination in a growth chamber at 26°C or 45°C, with 14 h light/10 h dark cycle.

Initial map-based resequencing (IMBR) of *PSL50*

Firstly, equal amounts of leaf blades from each of ten wild-type plants and ten *psl50*-type individual F_2 plants derived from *psl50*/80A90YR72 were collected for DNA extraction to form a wild-type (WT) DNA pool and a *psl50*-type DNA pool, respectively. These two DNA pools were subjected to preliminary linkage analysis of the mutation by genotyping 178 polymorphic simple sequence repeat (SSR) markers evenly covering 12 chromosomes. Subsequently, 40 *psl50*-type individual F_2 plants were genotyped to determine the primary physical location of *PSL50*. Approximately 5 mg fresh leaves from each of the four mutants (*psl50*, *M1*, *M2*, and *M3*) were collected to extract DNA (QIAGEN, Lot No. 145034200), and the DNAs were used for whole-genome resequencing at Majorbio company (Shanghai, China). The sequencing alignments were conducted on the cloud platform of Majorbio company (https://www.i-sanger.com/).

PSL50-GFP and CRISPR/Cas9 vector construction

The full CDS of *PSL50* were amplified from WT cDNA and cloned into pAN580 (GFP) vector (digested with *Spe*I restriction enzyme) with Gibson assembly strategy, and the GFP fluorescence signal was detected using Zeiss lsm710 confocal laser scanning microscope (Carl Zeiss, Inc., Jena, Germany). The CRISPR/Cas9 construct of *PSL50* was generated according to a previous report [10]. The genetic transformation was conducted by using embryogenic calli induced from the rice cultivar 'Kitaake' through Agrobacterium-mediated transformation method. Primers used in the study are listed in Table S1.

Measurement of MDA, H_2O_2 content and ion leakage rate

The contents of MDA and H_2O_2 were determined using the kits following the manufacturer's instructions (Nanjing Jiancheng Bioengineering Institute). For the ion leakage analysis, Leaves were cut into 0.5-cm pieces and 50 mg was weighed out precisely, then placed into 20 mL deionized water in a 50 mL tube, followed by vacuum treatment for 10 min, and incubated in a shaker with 100 rpm at 28°C for 30 min. The membrane ion leakage (value A) was measured using a DDS-307A conductivity meter (LeiCi, Hangzhou, China). Then, the samples were incubated in boiling water for 5 min to thoroughly release electrolytes. After the samples were cooled down to the room temperature, the final membrane ion leakage (value B) was measured. The value of membrane ion leakage was calculated by the formula A/B × 100%.

DAB and trypan blue staining

H_2O_2 accumulation and cell death were detected by DAB and trypan blue staining as described previously (He et al. 2018).

Real-time fluorescent quantitative PCR

Total RNA was extracted using a NucleoZOL Reagent Kit (MACHEREY-NAGEL, Düren, Germany) according to the manufacturer's protocol. RNA was reverse-transcribed using the ReverTra Ace qPCR RT Master Mix with genomic DNA (gDNA) Remover Kit (Toyobo, Osaka, Japan). Real-time fluorescent quantitative PCR (qRT-PCR) was carried out using the FastStar Essential DNA Green Master Kit (Roche, Basel, Switzerland) and performed on a Thermal Cycle Dice Real Time System (Takara, Kusatsu, Japan). For *PSL50* expression analysis, different parts of fully expanded flag leaves at the heading stage and different leaves of WT plants at the mature stage were sampled for RNA isolation. Rice *UBIQUITIN* (*LOC_Os03g13170*) was used as an internal control. Primers used in the study are listed in Table S4.

Protein extraction and immunoblot analysis

Leaf tissues (100 mg) were grounded in liquid nitrogen and placed into 600 μL extraction buffer (0.4 mM Tris-HCl, pH 7.5, 5 mM NaCl, 6.25 μM $MgCl_2$, 10 μM EDTA, 10 μM DL-dithiothreitol, 1% Triton X-100, 2% protease inhibitor) in a 2 mL tube, then incubated in a shaker at 80 rpm, 4°C for 30 min. Homogenates were centrifuged at 4°C with 10,000 *g* for 20 min, and the total supernatant proteins of wild-type and *psl50* were quantified into the same concentration by a BCA Protein Assay Kit (TIANGEN, Beijing, China). The quantified total proteins were denatured at 95°C for 10 min. Total proteins (10μ L) of wild-type and *psl50* were subjected to 12% (w/v) polyacrylamide sodium dodecyl sulfate-polyacrylamide gel electrophoresis (SDS-PAGE) and the resolved proteins were transferred onto a PVDF membrane. Antibodies used for immunoblot analysis were purchased from Agrisera (Vännäs, Sweden).

Declarations

Funding

This research was funded by the Central Public-interest Scientific Institution Basal Research Fund of China National Rice Research Institute (2017RG002-2).

Availability of Data and Materials

All data supporting the conclusions of this article are provided within the article (and its additional files).

Ethics Approval and Consent to Participate

Not applicable.

Consent for Publication

Not applicable.

Competing Interests

The authors declare that they have no competing interests.

Author details

State Key Laboratory of Rice Biology, China National Rice Research Institute, Chinese Academy of Agricultural Sciences, Hangzhou, 310006, China

Yan He: chinayanyan@163.com

Xiaobo Zhang: hello.xiaobo@163.com

Yongfeng Shi: shiyongfeng@caas.cn

Xia Xu: mailxuxia@163.com

Liangjian Li: liliangjian1994@163.com

Jian-li Wu: beishangd@163.com

Reference

Asada K (2006) Production and scavenging of reactive oxygen species in chloroplasts and their functions. Plant Physiol 141: 391–396

Bonifacio A, Carvalho FEL, Martins MO, Lima Neto MC, Cunha JR, Ribeiro CW, Margis-Pinheiro M, Silveira JAG (2016) Silenced rice in both cytosolic ascorbate peroxidases displays pre-acclimation to cope with oxidative stress induced by 3-aminotriazole-inhibited catalase. J Plant Physiol 201:17–27

Cui YM, Lu S, Li Z, Chen JW, Hu P, Zhu TQ, Wang X, Jin M, Wang XX, Li LQ, Huang SY, Zou BH, Hua J (2020) *CYCLIC NUCLEOTIDE-GATED ION CHANNELs* 14 and 16 promote tolerance to heat and chilling in rice. Plant Physiol 183:1794–1808

Fujii S, Toriyama K (2008) *DCW11*, *down-regulated gene 11* in CW-type cytoplasmic male sterile rice, encoding mitochondrial protein phosphatase 2c is related to cytoplasmic male sterility. Plant Cell Physio 49:633–640

Guan QJ, Liao X, He ML, Li XF, Wang ZY, Ma HY, Yu S, Liu SK (2017) Tolerance analysis of chloroplast *OsCu/Zn-SOD* overexpressing rice under NaCl and $NaHCO_3$ stress. PLoS One 12:e0186052

He Y, Li LJ, Zhang ZH, Wu JL (2018) Identification and comparative analysis of premature senescence leaf mutants in rice (*Oryza sativa* L). Int J Mol Sci 19: 140

He Y, Shi YF, Zhang X, Xu X, Wang HM, Li LJ, Zhang ZH, Shang HH, Wang ZH, Wu JL (2020) The OsABCI7 transporter interacts with OsHCF222 to stabilize the thylakoid membrane in rice. Plant Physiol 184:283–299

Ivanov AG, Velitchkova MY, Allakhverdiev SI, Huner NPA (2017) Heat stress-induced effects of photosystem I: an overview of structural and functional responses. Photosynth Res 133:17–30

Lee S, Lee HJ, Huh SU, Paek KH, Ha JHo, Park CM (2014) The *Arabidopsis* NAC transcription factor NTL4 participates in a positive feedback loop that induces programmed cell death under heat stress conditions. Plant Sci 227:76–83

Li GY, Zhang CX, Zhang GH, Fu WM, Feng BH, Chen TT, Peng SB, Tao LX, Fu GF (2020) Abscisic acid negatively modulates heat tolerance in rolled leaf rice by increasing leaf temperature and regulating energy homeostasis. Rice 13:18

Liang CZ, Wang YQ, Zhu YN, Tang JY, Hu B, Liu LC, Ou SJ, Wu HK, Sun XH, Chu JF, Chu CC (2014) OsNAP connects abscisic acid and leaf senescence by fine-tuning abscisic acid biosynthesis and directly targeting senescence-associated genes in rice. Proc Natl Acad Sci U S A 111:10013–10018

Lin AH, Wang YQ, Tang JY, Xue P, Li CL, Liu LC, Hu B, Yang FQ, Loake GJ, Chu CC (2012) Nitric oxide and protein S-nitrosylation are integral to hydrogen peroxide-induced leaf cell death in rice. Plant Physiol 158:451–464

Qiao YL, Jiang WZ, Lee JH, Park BS, Choi MS, Piao RH, Woo MO, Roh JH, Han LZ, Paek NC, Seo HS, Koh HJ (2010) *SPL28* encodes a clathrin-associated adaptor protein complex 1, medium subunit μ1 (AP1M1) and is responsible for spotted leaf and early senescence in rice (*Oryza sativa*). New Phytol 185:258–274

Saika H, Ohtsu K, Hamanaka S, Nakazono M, Tsutsumi N, Hirai A (2002) *AOX1c*, a novel rice gene for alternative oxidase; comparison with rice *AOX1a* and *AOX1b*. Genes Genet Syst 77:31–38

Samakovli D, Tichá T, Vavrdová T, Ovečka M, Luptovčiak I, Zapletalová V, Kuchařová A, Křenek P, Krasylenko Y, Margaritopoulou T, Roka L, Milioni D, Komis G, Hatzopoulos P, Šamaj J (2020) YODA-HSP90 module regulates phosphorylation-dependent inactivation of SPEECHLESS to control stomatal development under acute heat stress in *Arabidopsis*. Mol Plant 13:612–633

Sathe AP, Su X, Chen Z, Chen T, Wei XJ, Tang SQ, Zhang XB, Wu JL (2019) Identification and characterization of a spotted-leaf mutant *spl40* with enhanced bacterial blight resistance in rice. Rice 12:68

Shim Y, Kang K, An G, Paek NC (2019) Rice DNA-binding one zinc finger 24 (OsDOF24) delays leaf senescence in a jasmonate-mediated pathway. Plant Cell Physiol 60:2065-2076

Wang FB, Liu JC, Zhou LJ, Pan G, Li ZW, Zaidi SHR, Cheng FM (2016) Senescence-specific change in ROS scavenging enzyme activities and regulation of various SOD isozymes to ROS levels in *psf* mutant rice

leaves Plant Physiol Biochem 109:248–261

Wu HC, Bulgakov VP, Jinn TL (2018) Pectin methylesterases: cell wall remodeling proteins are required for plant response to heat stress. Front Plant Sci. 9:1612

Ye NH, Zhu GH, Liu YG, Li YX, Zhang JH (2011) ABA controls H□O□ accumulation through the induction of *OsCATB* in rice leaves under water stress. Plant Cell Physiol 52:689–698

Zhang BC, Liu XL, Qian Q, Liu LF, Dong GJ, Xiong GY, Zeng DL, Zhou YH (2011) Golgi nucleotide sugar transporter modulates cell wall biosynthesis and plant growth in rice. Proc Natl Acad Sci U S A 108:5110–5115

Zhang J, Chen LL, Xing F, Kudrna DA, Yao W, Copetti D, Mu T, Li W, Song JM, Xie W et al (2016) Extensive sequence divergence between the reference genomes of two elite *indica* rice varieties Zhenshan 97 and Minghui 63. Proc Natl Acad Sci U S A 113:5163–5171.

Zhao Y, Chan ZL, Gao JH, Xing L, Cao MJ, Yu CM, Hu YL, You J, Shi HT, Zhu YF, Gong YH, Mu ZX, Wang HQ, Deng X, Wang PC, Bressan RA, Zhu J (2016) ABA receptor PYL9 promotes drought resistance and leaf senescence. Proc Natl Acad Sci U S A 113:1949–1954

Figures

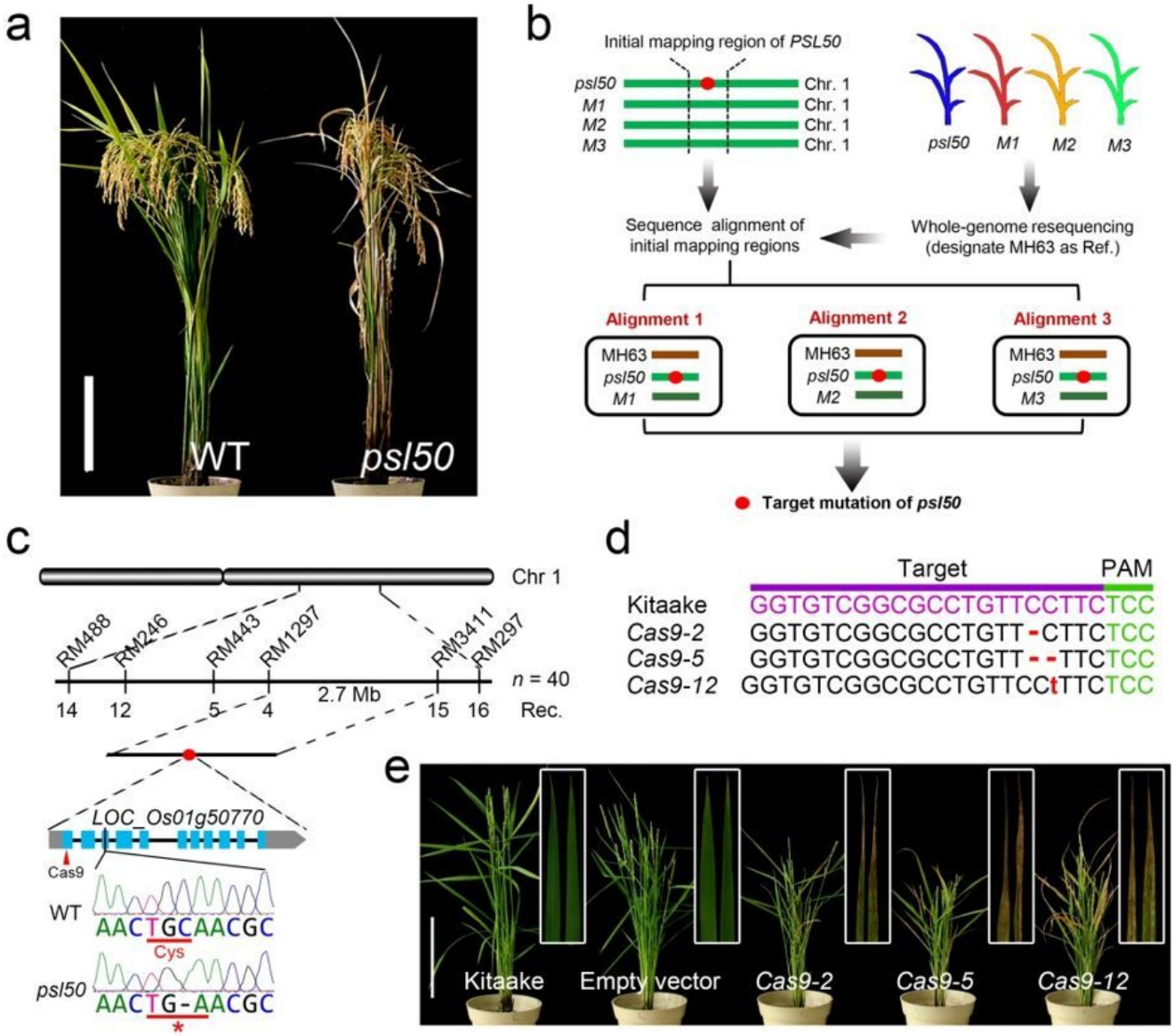

Figure 1

Identification of PSL50 by IMBR strategy. a Phenotype of WT and psl50 at the mature stage. Scale bar = 20 cm. b Identification of target mutation of psl50 by IMBR strategy. Red dot indicates the causative mutation responsible for the psl50 phenotype. c Initial mapping of PSL50 and verification of target mutation in PSL50. d Deletion and insertion mutation at the target site of 1st exon in three representative knockout lines generated by CRISPR/Cas9 in ‘Kitaake’ background. The Cas9-2, Cas9-5 and Cas9-12 lines are homozygous mutants carrying a 1-bp deletion, a 2-bp deletion and a 1-bp insertion on both homochrosomes, respectively. e Phenotype of three representative T0 knockout lines at the heading stage. Insets display magnified views of flag leaves. Kitaake-EV represents transgenic plant transformed with CRISPR/Cas9 empty vector. Scale bar = 20 cm.

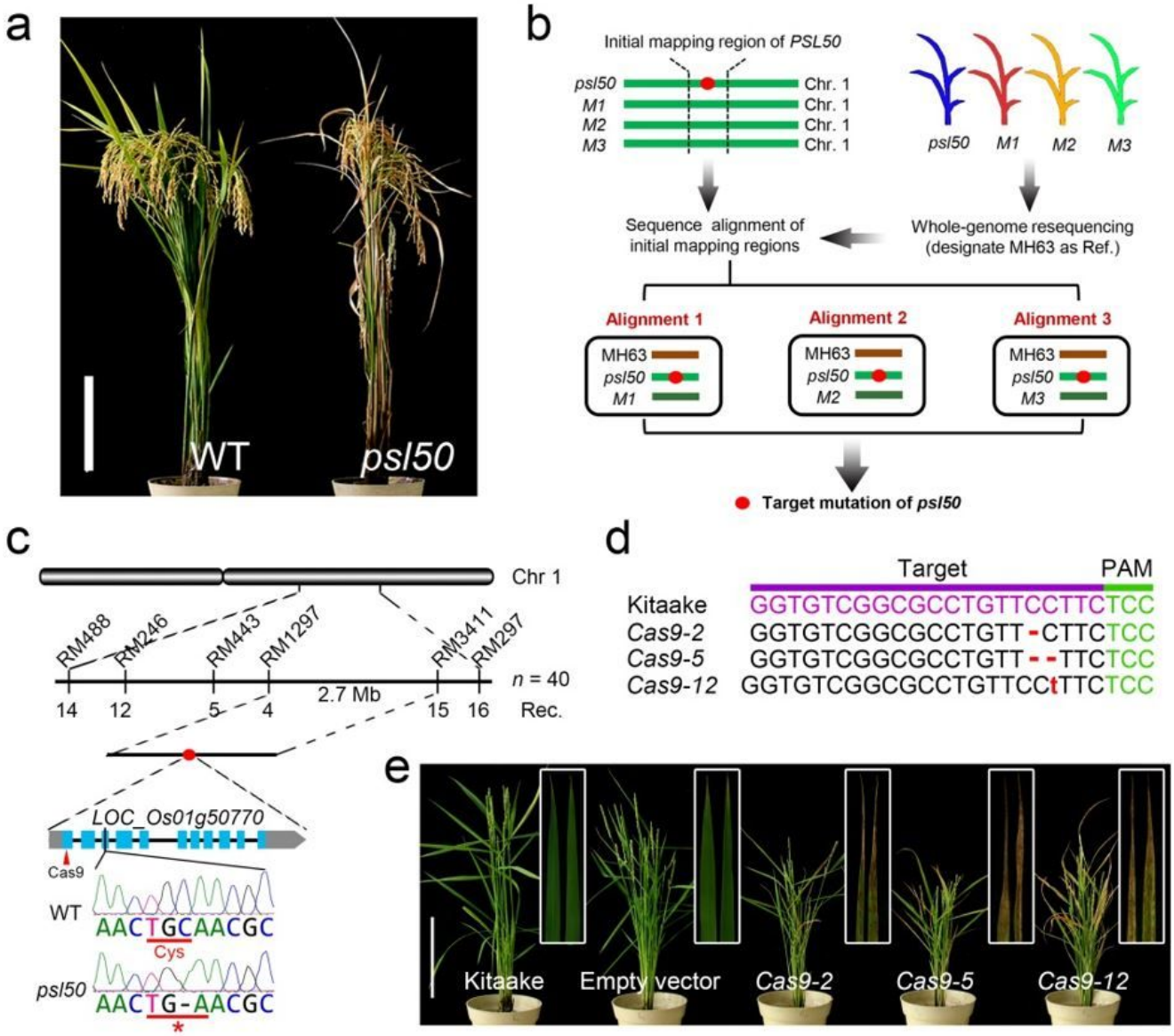

Figure 1

Identification of PSL50 by IMBR strategy. a Phenotype of WT and psl50 at the mature stage. Scale bar = 20 cm. b Identification of target mutation of psl50 by IMBR strategy. Red dot indicates the causative mutation responsible for the psl50 phenotype. c Initial mapping of PSL50 and verification of target mutation in PSL50. d Deletion and insertion mutation at the target site of 1st exon in three representative knockout lines generated by CRISPR/Cas9 in ‘Kitaake’ background. The Cas9-2, Cas9-5 and Cas9-12 lines are homozygous mutants carrying a 1-bp deletion, a 2-bp deletion and a 1-bp insertion on both homochrosomes, respectively. e Phenotype of three representative T0 knockout lines at the heading stage. Insets display magnified views of flag leaves. Kitaake-EV represents transgenic plant transformed with CRISPR/Cas9 empty vector. Scale bar = 20 cm.

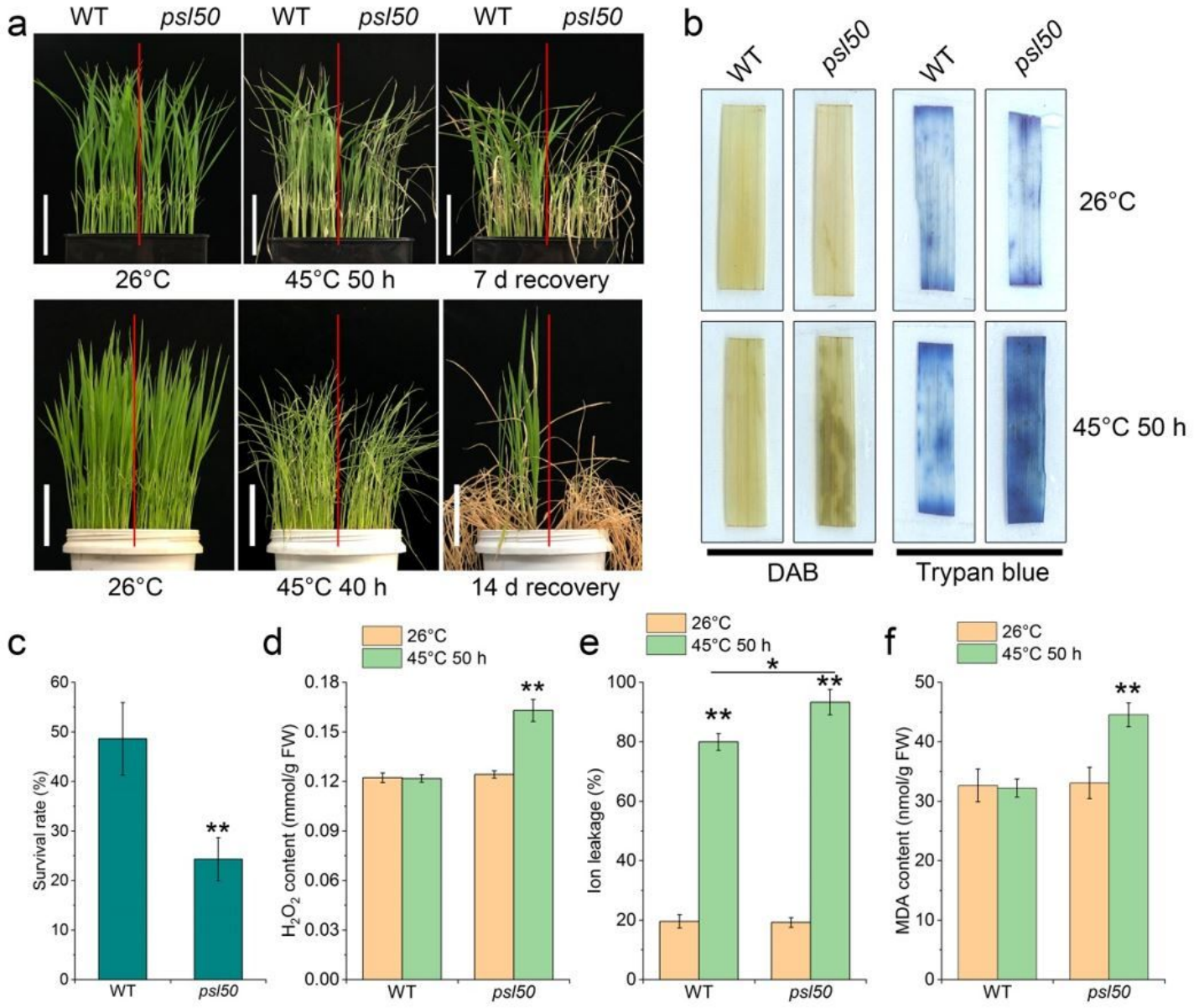

Figure 2

Effects of heat stress on psl50 and WT at the seedling stage. a Phenotypes of WT and psl50 seedlings under heat stress. Seedlings were hydroponically (upper row) or soil grown (lower row) at 26°C for 12 d and then treated at 45°C for 50 h or 40 h followed a recovery at 26°C. Scale bars = 5 cm. b DAB staining for H2O2 accumulation detection and trypan blue staining for cell death detection in the top 2nd leaves of hydroponically seedlings before and after heat treatment. c Survival rate of hydroponic WT and psl50 seedlings shown in a. d-f H2O2 content, ion leakage rate and MDA content in hydroponic WT and psl50 seedlings before and after heat treatment. Data are means ± SD (n = 3). Asterisks indicate significant difference by Student's t test (**P < 0.01 and *P < 0.05).

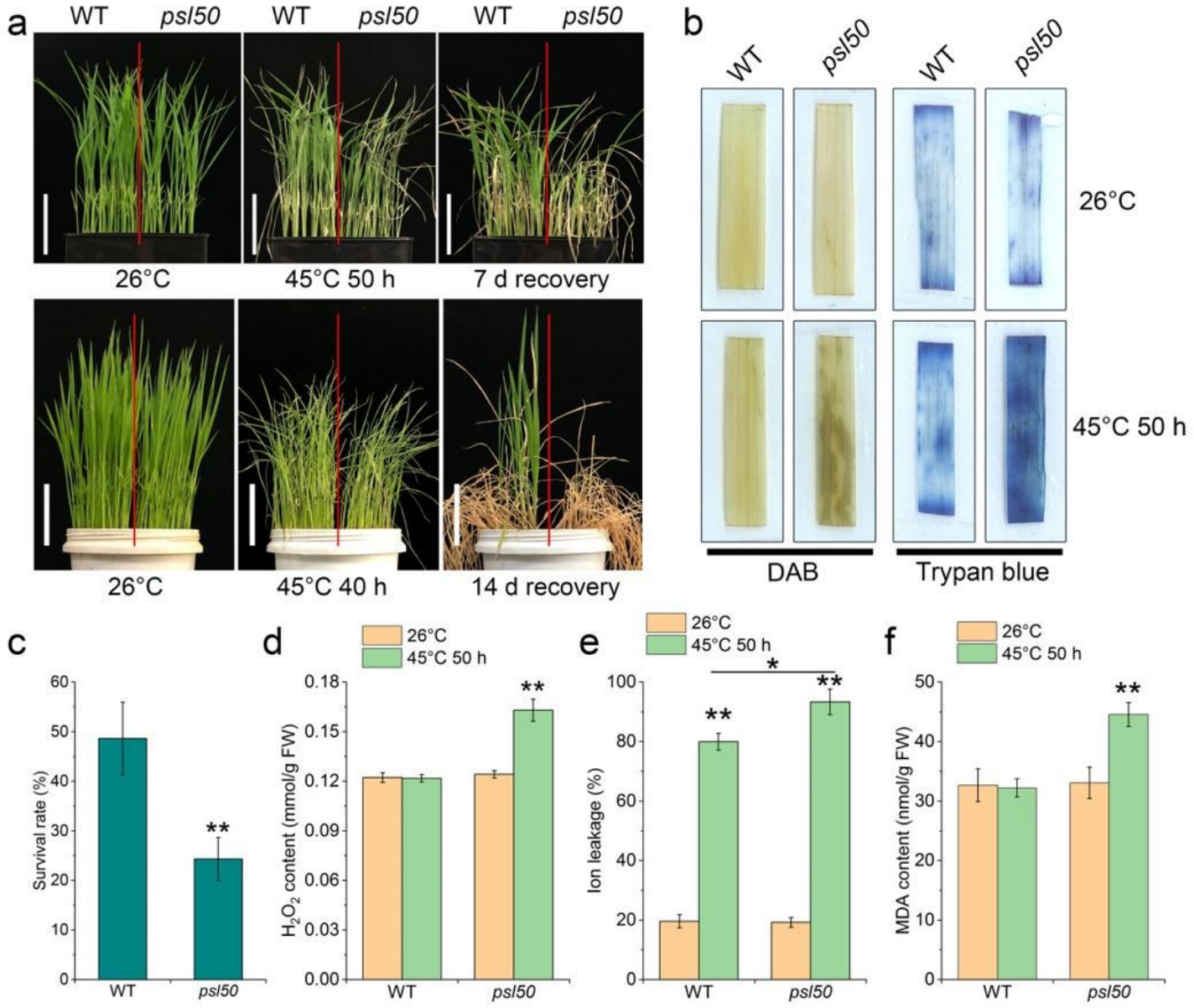

Figure 2

Effects of heat stress on psl50 and WT at the seedling stage. a Phenotypes of WT and psl50 seedlings under heat stress. Seedlings were hydroponically (upper row) or soil grown (lower row) at 26°C for 12 d and then treated at 45°C for 50 h or 40 h followed a recovery at 26°C. Scale bars = 5 cm. b DAB staining for H2O2 accumulation detection and trypan blue staining for cell death detection in the top 2nd leaves of hydroponically seedlings before and after heat treatment. c Survival rate of hydroponic WT and psl50 seedlings shown in a. d-f H2O2 content, ion leakage rate and MDA content in hydroponic WT and psl50 seedlings before and after heat treatment. Data are means ± SD (n = 3). Asterisks indicate significant difference by Student's t test (**P < 0.01 and *P < 0.05).

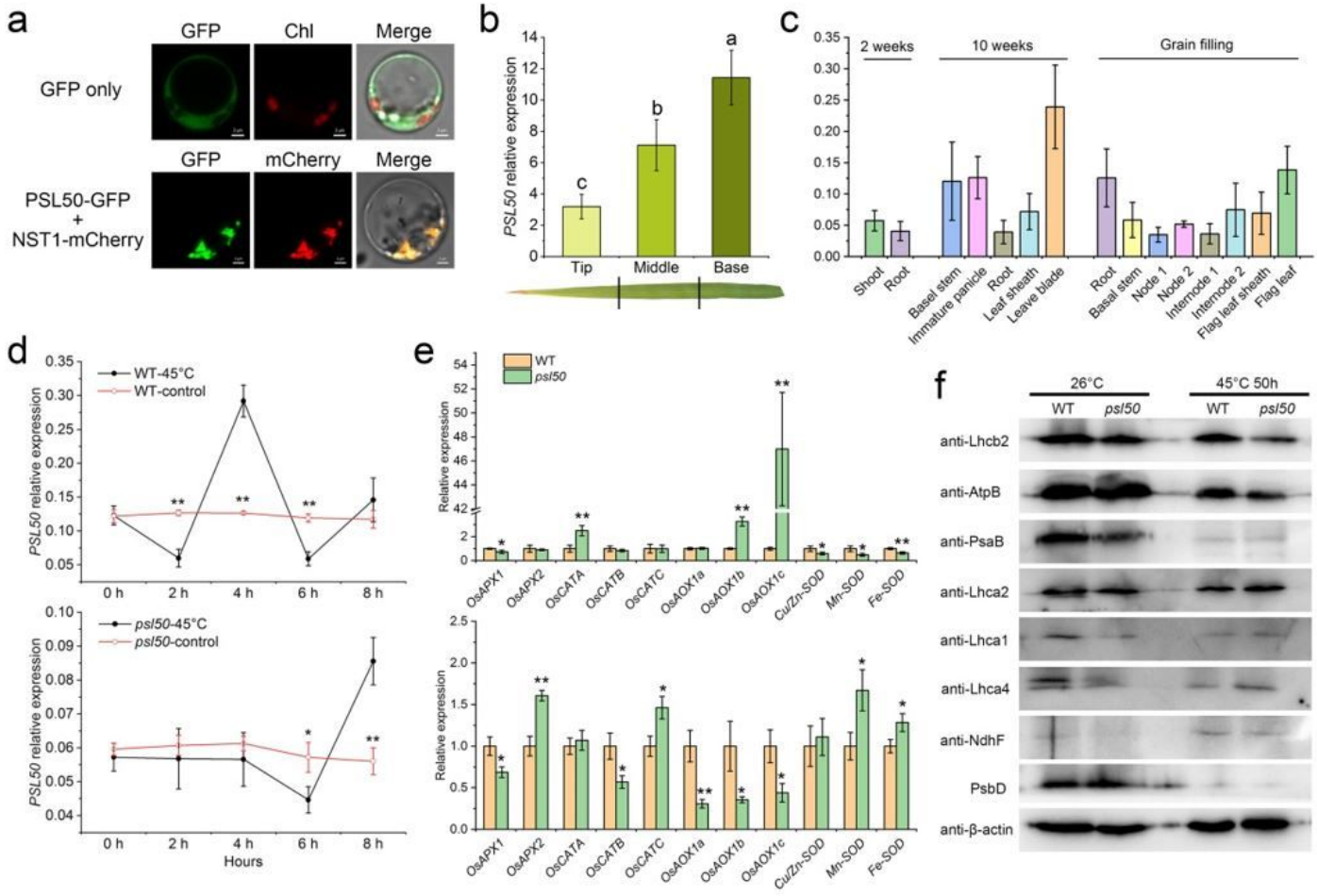

Figure 3

Effects of heat stress on psl50 and WT at the seedling stage. a Phenotypes of WT and psl50 seedlings under heat stress. Seedlings were hydroponically (upper row) or soil grown (lower row) at 26°C for 12 d and then treated at 45°C for 50 h or 40 h followed a recovery at 26°C. Scale bars = 5 cm. b DAB staining for H2O2 accumulation detection and trypan blue staining for cell death detection in the top 2nd leaves of hydroponically seedlings before and after heat treatment. c Survival rate of hydroponic WT and psl50 seedlings shown in a. d-f H2O2 content, ion leakage rate and MDA content in hydroponic WT and psl50 seedlings before and after heat treatment. Data are means ± SD (n = 3). Asterisks indicate significant difference by Student's t test (**P < 0.01 and *P < 0.05).

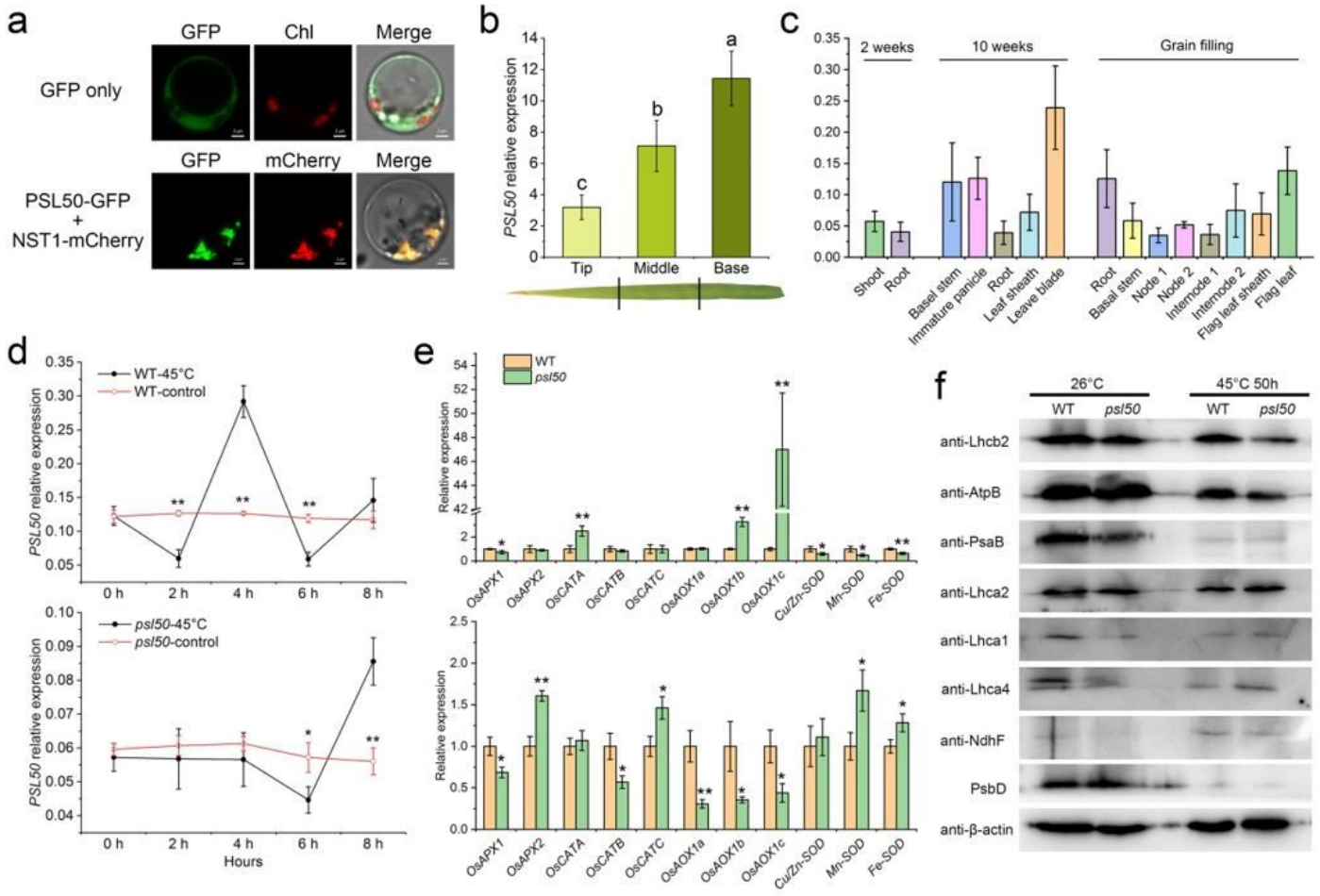

Figure 3

Effects of heat stress on psl50 and WT at the seedling stage. a Phenotypes of WT and psl50 seedlings under heat stress. Seedlings were hydroponically (upper row) or soil grown (lower row) at 26°C for 12 d and then treated at 45°C for 50 h or 40 h followed a recovery at 26°C. Scale bars = 5 cm. b DAB staining for H2O2 accumulation detection and trypan blue staining for cell death detection in the top 2nd leaves of hydroponically seedlings before and after heat treatment. c Survival rate of hydroponic WT and psl50 seedlings shown in a. d-f H2O2 content, ion leakage rate and MDA content in hydroponic WT and psl50 seedlings before and after heat treatment. Data are means ± SD (n = 3). Asterisks indicate significant difference by Student's t test (**P < 0.01 and *P < 0.05).

Supplementary Files

This is a list of supplementary files associated with this preprint. Click to download.

- Additionalfile1.rar
- Additionalfile1.rar
- Additionalfile2.rar

- Additionalfile2.rar